Stanford Exploration Project, Report 67, January 13, 1998, pages 1–44

Traveltime inversion of a cross-well dataset for elliptically anisotropic media

Carlos A. Cunha Filho[1]

keywords: *inversion, modeling, traveltime, elastic*

ABSTRACT

Using the paraxial elliptical approximation for the dispersion relation around a horizontal axis, I applied a homogeneous and a layered traveltime inversion scheme to a common-receiver, multi-component, cross-well dataset. Each wave-type was inverted independently for the two parameters that describe the elastic model for media with elliptical anisotropy. The layered inversion scheme decomposes the model into a set of symmetric and anti-symmetric square functions. Results of the homogeneous inversion for the P and SV waves show a considerable degree of elliptical anisotropy. Even with the absence of SH information we were able to obtain four of the five transverse isotropic elastic parameters. Although the insufficient coverage of this specific dataset compromises the uniqueness of the solution, the first iterations of the layered scheme represent at least one resolution-step ahead of the homogeneous results.

INTRODUCTION

The inversion problem in transversely isotropic media consists of the estimating 5 elastic constants for each point of the model space, using the recorded wavefield. For this particular symmetry, the dispersion relation for the SH wave is exactly elliptical, while the other two wave types obey a dispersion relation that depends on all 5 elastic parameters. Using an elliptic approximation for the dispersion relations of P and SV waves can considerably simplify the inversion problem (Levin, 1978, Muir and Dellinger, 1985) because the number of independent parameters per wave type is reduced to 2. This method also provides a fast way of testing the validity of the axial-symmetry, by comparing the independently estimated parameters of SH and SV waves.

Karrenbach (1989) proposed a practical scheme to invert cross-well data for the case of a homogeneous, transversely isotropic medium, using the elliptic approximation and traveltime information for each component. I applied this homogeneous

[1]**email:** not available

inversion scheme to a three-component cross-well dataset recorded by Western Geophysical. Unfortunately, it was not possible to detect a coherent SH arrival. Consequently, we were able to obtain only four elastic parameters from the estimated elliptic parameters. As an extension to the homogeneous inversion, I have derived a scheme for the more general case of a horizontally layered model and tested it in a synthetic dataset. In this scheme, the model is represented by a superposition of a basis set of symmetric and anti-symmetric square functions. When applied to the cross-well data, the layered inversion scheme generates a stable solution with associated traveltimes that show a better fit to the data than the homogeneous results. However, the insufficient amount of data used compromises the reliability of a higher resolution estimation. Nevertheless, the results obtained with the first few iterations (corresponding to the low frequency components of the model) can be still considered a reliable improvement in the resolution of the model.

THE HOMOGENEOUS INVERSION SCHEME

For elliptically anisotropic media, that is, media in which the group velocity V has an elliptical dependence on the angle of energy propagation ϕ, such that

$$\frac{(V\cos\phi)^2}{V_x} + \frac{(V\sin\phi)^2}{V_z} = 1, \tag{1}$$

the relation between group and phase velocities and angles is given by a closed analytical form (Levin, 1978):

$$\frac{v(\theta)}{V(\phi)} = \cos(\phi - \theta) \tag{2}$$

$$\tan(\phi) = \left(\frac{V_z}{V_x}\right)^2 \tan(\theta) \tag{3}$$

where v and θ are the phase velocity and angle, respectively. Equation (1) also represents an elliptical dispersion relation, since $V\sin\phi = K_x/\omega$ and $V\cos\phi = K_z/\omega$. It turns out that elasticity theory predicts this elliptical dependence only for S_H in a transverse isotropic symmetry, or for all wave types in the trivial case of isotropic material where the ellipse becomes a circle. However, the use of an elliptical approximation for the dispersion relation can considerably simplify the problem of estimating the elastic parameters from the recorded wavefields.

If we consider a source and a receiver separated by a vertical distance z and a horizontal distance x, the traveltime t predicted by equation (1) is

$$t^2 = M^x\, x^2 + M^z\, z^2. \tag{4}$$

The relation between the slownesses squared (or sloth) M^x and M^z [2] that best fits our data and the true vertical and horizontal sloths of the medium M^v and M^h respec-

[2]The reason I am using superscripts here is to avoid excessive subscript indexing later.

tively will depend on the specific geometry in which the data was collected. For an usual surface-seismic geometry, equation (4) correspond to a paraxial approximation around the vertical axis. In this case, M^x corresponds to the estimated normal-moveout (NMO) sloth, while $M^z\, z^2$ is the vertical traveltime. If z is unknown, then M^z is an arbitrary factor that cannot be estimated (Dellinger and Muir, 1985).

If both distances, x and z, are known it is possible to estimate both sloth parameters by fitting the data to equation (4). For surface seismic surveys the estimated M^z will be close to the vertical sloth M^v, whereas for a cross-well geometry the estimated M^x will be close to the horizontal sloth M^h. Karrenbach (1989) described a scheme to estimate these two sloth parameters using traveltime data from the three wave types, for the case of a homogeneous medium. He also derived the relations between these parameters and the elastic constants corresponding to a transversely isotropic symmetry, for the specific case of a cross-well geometry.

HORIZONTALLY LAYERED INVERSION

While equation (4) is linear in t^2 for the homogeneous case, the introduction of layers disrupts this linearity because here we must add traveltimes and not traveltimes squared. This non-linearity represents a problem if the model space is composed of layers (or cells), because the excessive number of unknowns brings not only a prohibitive cost, but also an increasing degree of instability in the solution as the number of model parameters increase. One possible solution is to linearize the problem, and solve it in an iterative scheme. Another is to decompose the model into an orthogonal set of functions and solve for each component independently.

I use here an approach that is closely related to this second form, but which substantially simplifies the forward computations in the initial iterations. Moreover, because of the way it builds the solution– by the introduction of successive degrees of complexity, this method is highly stable.

Similarly to the Fourier decomposition, the method represents the sloth model as composed by the superposition of two sets of oscillatory functions (one set comprised of symmetric functions and the other comprised of anti-symmetric functions), plus a constant factor that accounts for the average-model

$$\mathbf{M} = c + \sum_{i=1}^{N} a_i\, \mathcal{S}_i + \sum_{i=1}^{N} b_i\, \mathcal{C}_i. \tag{5}$$

The basis functions $\mathcal{S}_i$ and $\mathcal{C}_i$ are *sine*-like and *cosine*-like square waves with an integer number of cycles i, with a fixed length corresponds to the total depth interval spanned by the model. I will not address here the discussion about the orthogonality and completeness of the basis set of functions and the space spanned by them, but rather emphasize their practicality as model generators in the inversion scheme that follows.

The first step of the method corresponds to the homogeneous inversion described in the previous section, and it accounts for the component c in equation (5). Next, an iterative process is applied, in which the *ith* iteration corresponds to a perturbation in the solution of the previous iteration; the perturbation is formed by a linear combination of the two basis functions of order i (that is, i cycles). Figure **??** shows how the perturbations in the model are constructed for the first two iterations. As explained in the figure caption, the actual parameters to be estimated at each iteration are not a and b, but dM_1 and dM_2, which are directly related to the perturbations in each layer. Since we must consider perturbations in M^x as well as in M^z, the number of independent parameters to be estimated at each iteration will always be four: dM_1^x, dM_2^x, dM_1^z, and dM_2^z.

Differently from the Fourier decomposition, here the number of points (layers) describing the model is not fixed for the retrieval of all the frequency components, but instead increases proportionally to the sequential number of the iteration. At each iteration, the total number of layers is four times the sequential number of the iteration. The solution is constructed in successive degrees of resolution, which results in a highly stable method, despite the use of a non-linear optimization algorithm.

The objective function to be minimized at each iteration is

$$\mathcal{F} = \sum_{i=1}^{N} \sum_{j=J_i}^{L_i} \left(t_{ij} - t'_{ij} \right)^2 , \tag{6}$$

where N is the number of shots, J_i and L_i refer to the extreme receivers of shot number i, t_{ij} is the measured traveltime corresponding to shot i and receiver j, and t'_{ij} is the traveltime predicted by the perturbed model. Using the straight-rays approximation, the predicted traveltime is given by

$$\begin{aligned} t'_{ij} \;=\; & \sum_{k=K_i}^{K_j} o_k \sqrt{(M_k^x + s_k dM_1^x) x_{ijk}^2 + (M_k^z + s_k dM_1^z) z_{ijk}^2} + \\ & e_k \sqrt{(M_k^x + s_k dM_2^x) x_{ijk}^2 + (M_k^z + s_k dM_2^z) z_{ijk}^2}, \end{aligned} \tag{7}$$

where o_k, e_k, and s_k are defined as

$$o_k = \frac{1 - (-1)^k}{2}, \qquad e_k = \frac{1 + (-1)^k}{2}, \qquad s_k = (-1)^{(k+3)/2}. \tag{8}$$

In equation (7) the subscript k is the number of a particular layer (for this particular iteration), while K_i and K_j correspond to the layers where the source i and receiver j are localized respectively. The horizontal x_{ijk} and the vertical z_{ijk} distances traveled by the ray that links source i to receiver j inside the layer k are constants for all but the first and last layers.

I applied the method to a synthetic dataset corresponding to a single isotropic horizontal layer immersed in an also isotropic background. The data consists of traveltimes from 20 shots localized in one well, each recorded by 51 receivers localized

in the other well. The space between adjacent sources was 5 times as larger as the distance between adjacent receivers. The layer thickness and the distance between wells were 3.33 and 3.6 times the distance between sources, respectively. Figure 1 shows the original and the retrieved models, as well as the partial result of each iteration.

The final results for V_x and V_z are close enough to the original model, if we consider the resolution limit associated with the specific acquisition-parameters and geometry. As expected, the part of the model that corresponds to V_x converges faster, and for a better solution, than the part that corresponds to V_z. The layer thickness in the last iteration is about 3/5 the source interval.

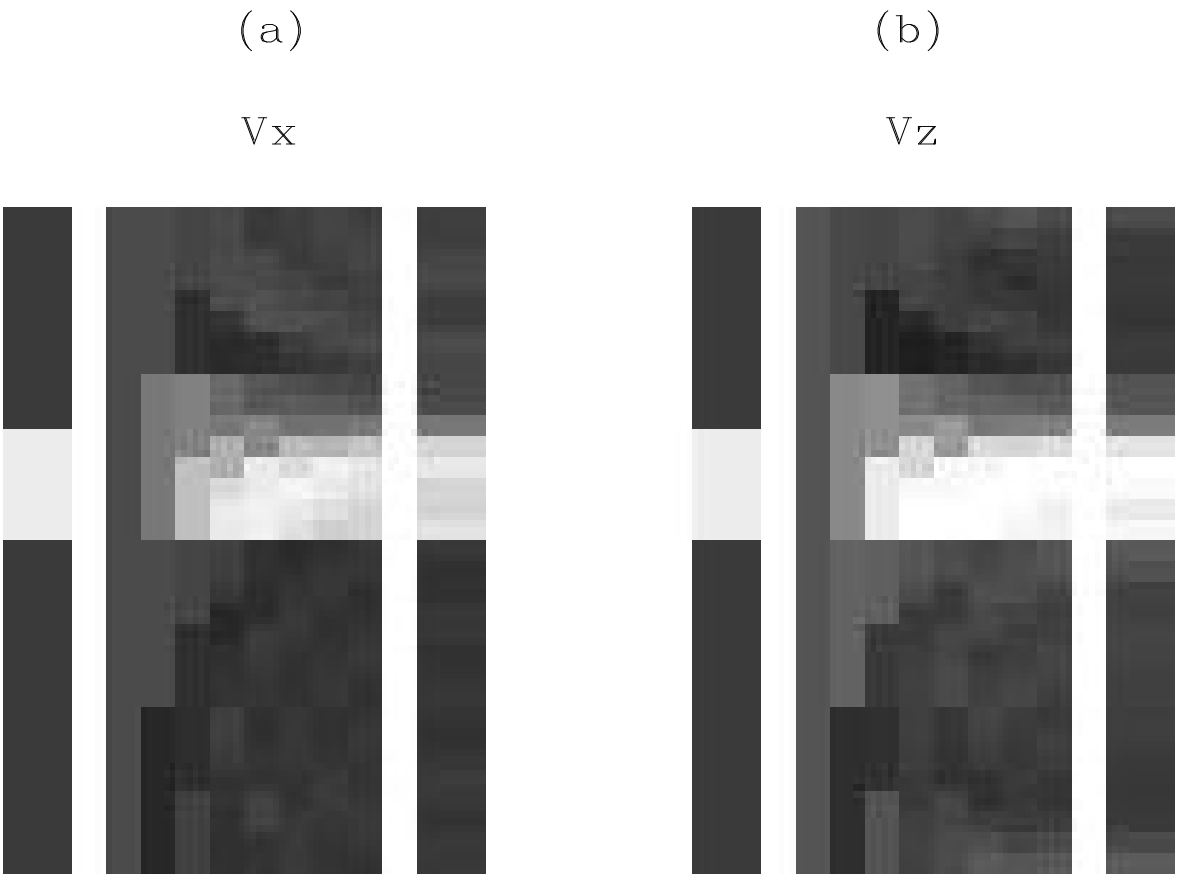

Figure 1: Original synthetic model and successive results of the layered inversion scheme. *(a)* Is the V_x part of the model, while *(b)* is the $V - z$ part. In both cases the extreme left column is the original model and the extreme right is the result of the $8th$ iteration (32 layers); they are displayed with a vertical exaggeration of 1.5 relative to the actual dimensions. The intermediary columns correspond to the results of the homogeneous inversion and all the successive iterations (1-7). They are displayed with half the horizontal width of the extremes for purposes of compactness. carlos2-hetmod [NR]

RESULTS

The method described in the previous section was applied to a cross-well dataset recorded by Western Geophysical with a extensive source that was able to generate a high energy SV wavefield. The part of the data considered here was acquired with a fixed three-component receiver localized in one well, and 61 source positions in another well with a horizontal offset of 1707 feet from the first well. The distance between sources was approximately 100 feet for the first 38 shots and 50 feet for the remaining shots.

A subgroup was organized at SEP to work with these data, and several processes were applied before picking the traveltimes that I used in the inversion. Cole and Karrenbach (1990) decomposed the data into the three fundamental wavefields P, SV and SH, using an estimation of the P-wave particle motion direction. They then used the decomposed data to estimate the P and SV wavelets. The SH component did not show a coherent arrival that could be objectively associated to an SH arrival. This result was expected, since the source was not designed to vibrate around the vertical axis, and was therefore not appropriate for the generation of SH waves. We had some hope however, that a weak SH wavefield could be generated in connection with the heterogeneities of the earth in the vicinity of the source. Vanian (1990) used the estimated wavelets to deconvolve the data and tried to detect, in the velocity space, a coherent signal that could be identified with the SH arrival. At present, we are still unable to identify a consistent arrival that can be objectively interpreted as an SH wave, assuming that such a wave-type was generated at all.

To select the traveltimes, I used an automatic-picking algorithm, which was based on an properly weighted correlation between the estimated wavelets and each trace of the decomposed wavefield. Figure 2 shows the results of the homogeneous and layered inversions of the P and SV traveltimes. Both wave-types show a considerable degree of elliptic anisotropy (more than 15 percent in average). The results of the layered inversion for V_x are substantially more stable than the ones for V_z, which starts to show an oscillatory behavior at iterations of high order. If we look however at the fourth iteration (dotted lines) we can see some consistence between V_z^P, V_x^P and V_z^{SV}, for the region above 3500 feet.

Using the results of the inversion I calculated (except for an unknown density factor) 4 of the elastic parameters that characterize a transversely isotropic medium. This evaluation was based in a paraxial approximation of the transverse isotropic dispersion relations, around the horizontal axis (Karrembach, 1989). Since the density is unknown, I have decided to express the results, in terms of the square-roots of parameter/density ratios to keep the velocity dimension. The paraxial fitting relations are

$$v_{11} = \sqrt{\frac{c_{11}}{\rho}} = V_x^P \qquad v_{33} = \sqrt{\frac{c_{33}}{\rho}} = \sqrt{2\Delta_z - (V_x^P)^2} \tag{9}$$

$$v_{44} = \sqrt{\frac{c_{44}}{\rho}} = V_x^{SV} \qquad v_{13} = \sqrt{\frac{c_{13}}{\rho}} = \sqrt{\sqrt{(\Delta_z + \Delta_x)\Delta_x} - (V_x^P)^2} \tag{10}$$

where

$$\Delta_x = (V_x^P)^2 - (V_x^{SV})^2 \qquad \text{and} \qquad \Delta_z = (V_z^P)^2 - (V_z^{SV})^2.$$

Figure 3 shows these 4 parameters evaluated with the results of the homogeneous and layered inversion. For the homogeneous case I present two results: one obtained with the use of all the receivers, and the other with a limited number of receivers (30 degrees of aperture) to assure the validity of the paraxial approximation. For the layered inversion I used the solution of the fourth iteration since V_x is more stable here than at later iterations.

I must observe, however, that the results of the heterogeneous inversion are not completely reliable for this particular dataset, because only traveltimes from a single receiver were available, and therefore, many different models could fit the data equally well.

Although we cannot trust the degree of resolution expressed by the results of the layered inversion, the traveltimes predicted by the heterogeneous model fit the measured traveltimes better than the traveltimes predicted by the homogeneous model, as shown in Figure 4. The constant-time step that appears at trace 25 corresponds to two shots at the same location.

CONCLUSIONS

The amount of new information that can be collected with the use of multi-component cross-well data such as that analyzed here seems worth the extra cost associated with this kind of survey. Using a single common-receiver gather to invert traveltime data strongly restricted the resolution of the retrieved model. Nevertheless, the low-frequency components of the model independently estimated for each wave type showed a reasonable consistency. Furthermore, the results obtained with the proposed scheme in synthetic data indicate that the use of a more complete real dataset (with several receiver positions) will allow for a reliable layered anisotropic inversion using the elliptic approximation.

Still to be analyzed are the correlation between traveltime and particle-motion direction and the information that can be obtained from it. The absence of SH information restricts the use of the elliptical inversion for estimating transversely isotropic elastic parameters. Consequently some further effort should be made to introduce a rotational mode in the source vibration pattern, and to uncover a weak uncoherent SH energy from the available data.

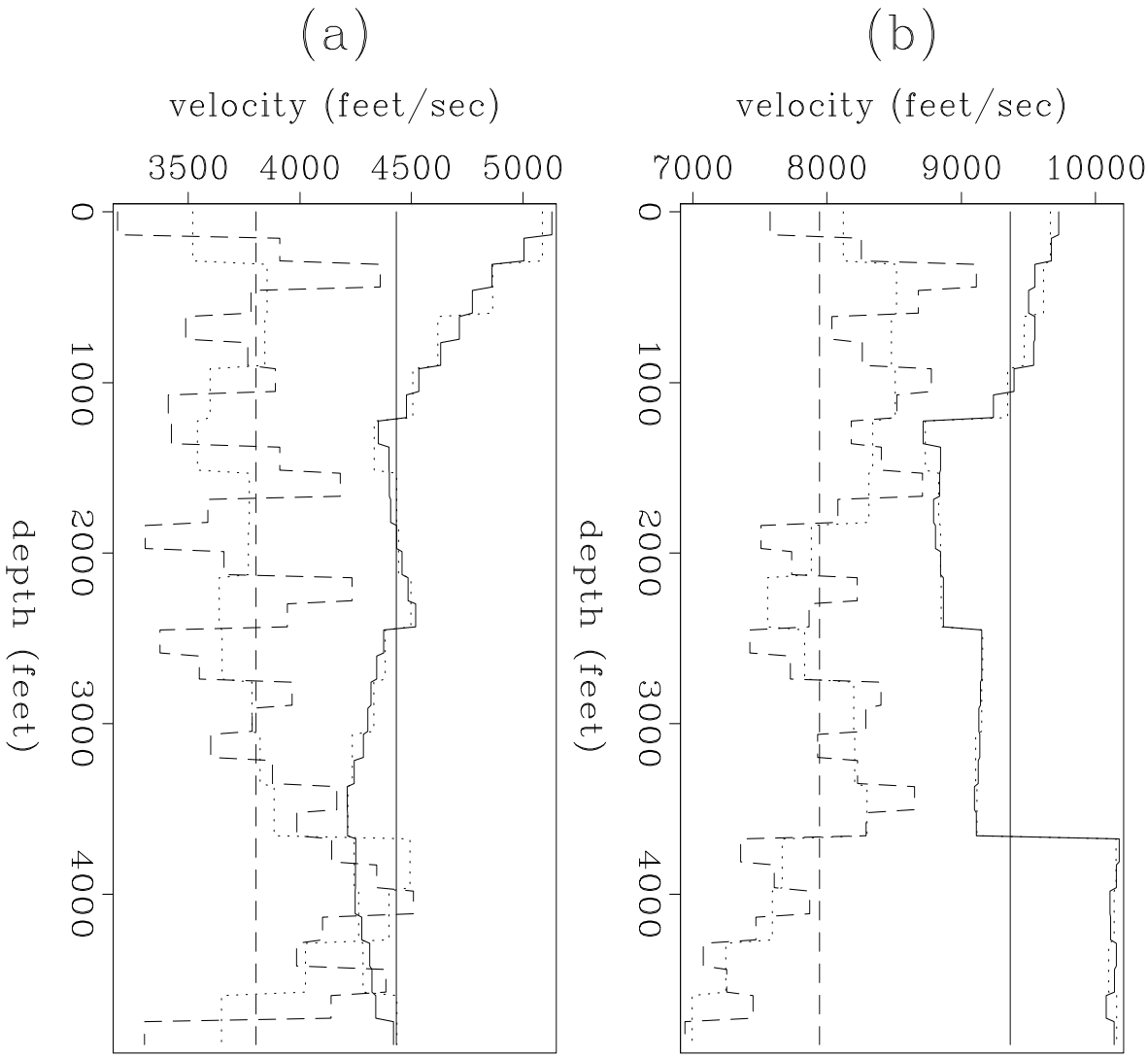

Figure 2: *(a)* represents the inversion results for the SV arrivals and *(b)* the results for the P arrivals. In both cases the continuous lines refer to the homogeneous and final results for V_x, the dashed lines refer to the homogeneous and final results for V_z, and the dotted lines correspond to the results of an intermediary iteration for both V_x and V_z. Depth zero does not correspond to the earth's surface. carlos2-invpsv [NR]

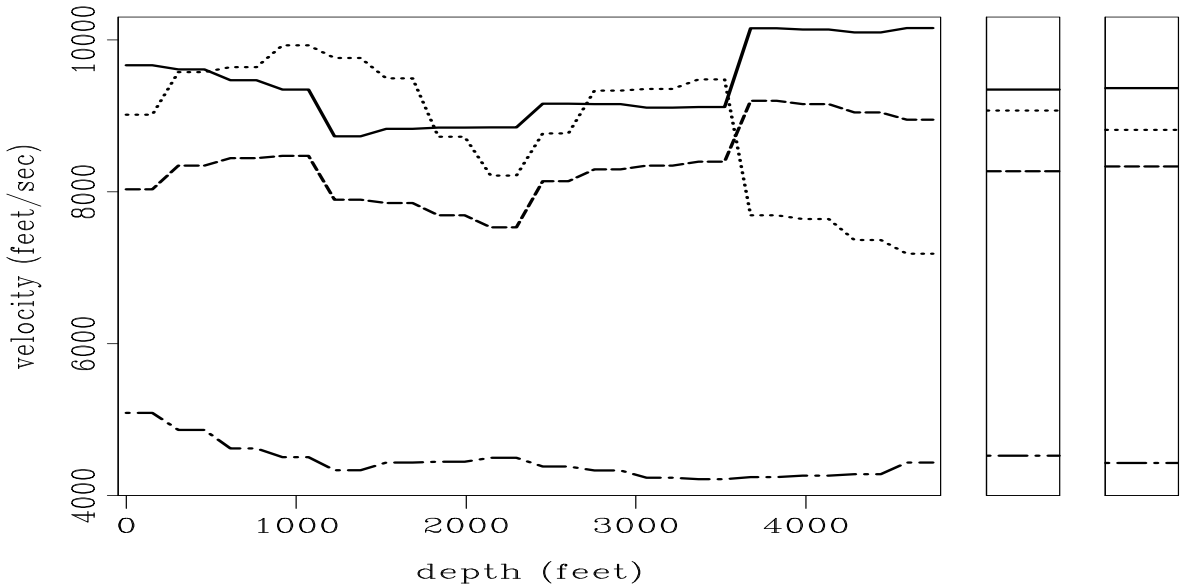

Figure 3: The four redimensioned elastic parameters obtained from the layered inversion are represented in the left panel. The two other panels correspond to the results of homogeneous inversion using traveltime information from: a restricted angular aperture of 30 degrees (center), and the complete 66 degrees aperture (right). The convention for the display are: v_{11} (continuous line), v_{33} (dotted line), v_{13} (dashed line), and v_{44} (dotted-dashed line). carlos2-elaspar [NR]

ACKNOWLEDGMENTS

I would like to thank my colleagues at the SEP cross-hole sub-group for the many interesting discussions and suggestions, and in special Francis Muir, who is behind most of the ideas discussed in this work.

REFERENCES

Cole, S., and Karrenbach, M., 1990, Rotation and wavelet estimation using cross-hole data, SEP–**67**, 31-36.

Dellinger, J., and Muir, F., 1985, Axisymmetric anisotropy I: Kinematics: SEP–**42**, 1-23.

Karrenbach, M., 1989, Velocity and Q in transverse isotropic media: SEP–**60**, 271-283.

Levin, K.L., 1978, The reflection, refraction, and diffraction of waves in media with an elliptical velocity dependence: Geophysics, **43**, 528-537.

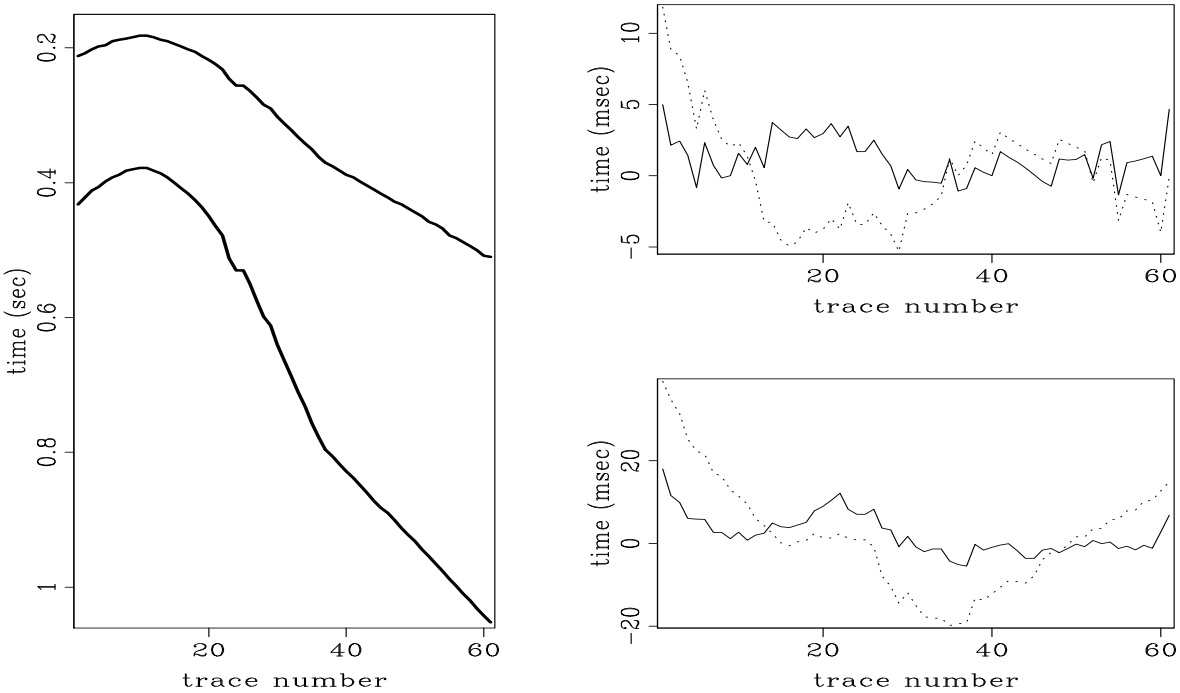

Figure 4: The panel on the left shows the traveltimes for P (top line) and SV (bottom line) picked from the data. The panels on the right show the residual traveltimes that correspond to the homogeneous inversion (dotted lines) and layered (continuous lines) inversion. The top panel corresponds to P, and the bottom panel to SV. carlos2-fittime [NR]

Muir, F., and Dellinger, J., 1985, A practical anisotropic system: SEP–**44**, 55-58.

Vanian, L., 1990, Deconvolution of cross-hole data, SEP–**67**, 37-38.